Progress In Electromagnetics Research Letters, Vol. 62, 117–123, 2016

Design of Miniaturized and Ultrathin Absorptive/Transmissive Radome Based on Interdigital Square Loops

Bo Yi*, Liang Yang, and Peiguo Liu

Abstract—This paper designs a miniaturized and ultrathin absorptive/transmissive radome based on interdigital square loops. The thickness of designed radome is only 4.5 mm. The period of the radome is 10 mm, which is $\lambda/17.5$ (λ corresponding to the wavelength of center frequency of passband). In order to verify the transmission and reflection properties, a prototype is fabricated. Its effectiveness is verified by both synthetic experiments and measurements in the anechoic chamber. Furthermore, the oblique incidents are also evaluated for both the transmission coefficients and reflection coefficients.

1. INTRODUCTION

Radar radome based on frequency selective surface(FSS) can be used not only to protect antenna from physical damage caused by wind or rain, but also to reduce the radar cross section(RCS) by reflecting the incident wave to unimportant direction or absorbing the incident wave [1]. As multistatic radar systems emerge, the reflecting signal may also be detected and stealth based on reflection faced great challenges. Desired stealthy technology should absorb the incident wave and not hamper the normal operation of antenna.

A radome proposed in a US patent in 1995 solves the above problem [2]. As the patent states, the radome would provide a passband at given frequency and absorb wave in absorbing band. The radome presents an effective way to stealth. Nevertheless, this patent only gives the qualitative working principle of the radome, and no quantitative results are presented.

Costa and Monorchio realized the functions in the above patent using three-layered structure, which contains resistive FSS, substrate and passband FSS. The absorptive/transmissive radome in [1] possesses good transmission performance and well absorbing property. Liu et al. designed another invisible radome with lumped resistors and also verified the performance of the radome using experiments [3]. Chen and Fu studied the influence on performance of antenna using the structure designed in [4] and improved the structure by replacing convoluted slots with another miniaturized element as bandpass FSS [5]. The improved structure solved the problems of grating lobes successfully. Zhou et al. designed another absorptive/transmissive radome using magnetic material and verified its properties experimentally [6]. The period of bandpass FSS of above designs was large, and grating lobes might appear in the absorbing band [1, 3, 4]. The unequal period between resistive and bandpass FSS may lengthen the simulated time in process of radome designing [1, 3–5].

Interdigitating the unit cells at the common boundary of adjacent unit cells of FSSs is an efficient technique for miniaturized FSSs and is firstly presented in [7], which was used for square spiral elements [8].

In this paper, a miniaturized and ultrathin radome based on the interdigital square loops was designed. Compared with the radome in [3–6, 9], the proposed radome owns smaller unit cells. The

Received 2 August 2016, Accepted 14 September 2016, Scheduled 27 September 2016

* Corresponding author: Bo Yi (ybtlqyb@163.com).

The authors are with the College of Electronic Science and Engineering, National University of Defense Technology, Changsha, Hunan, China.

period of resistive FSS is equal to that of bandpass FSS, which may reduce the simulated time greatly and shift the grating lobes out of absorbing band [1]. The profile of radome is only 4.5 mm, and its absorbing band is more than 10 GHz. Most importantly, the miniaturized and simplified design procedures do not result in performance loss, which has been verified by both simulated and experimental measurements.

This paper is organized as follows. The equivalent circuit is presented in Section 2. The designed radome is proposed, and numerical simulated results with the aid of CST are given in Section 3. Then, a prototype is fabricated, and its transmission and absorbing properties are verified by experiments in Section 4. Finally, the conclusions are drawn in Section 5.

2. ANALYSIS OF EQUIVALENT CIRCUIT

The absorptive/transmissive radome is often composed of resistive FSS, substrate and bandpass FSS. According to [10, 11], the simplest equivalent circuit of resistive FSS may be represented by a series connection of resistance R_0, capacitance C_0 and inductance L_0 and that of bandpass FSS by a parallels connection by capacitance C_1 and inductance L_1. The substrate may be seen as a transmission line with characteristic impedance Z_ξ. Based on the above analysis, the equivalent circuit of radome may be expressed as Fig. 1, where Z_0 represents the characteristic impedance of free space.

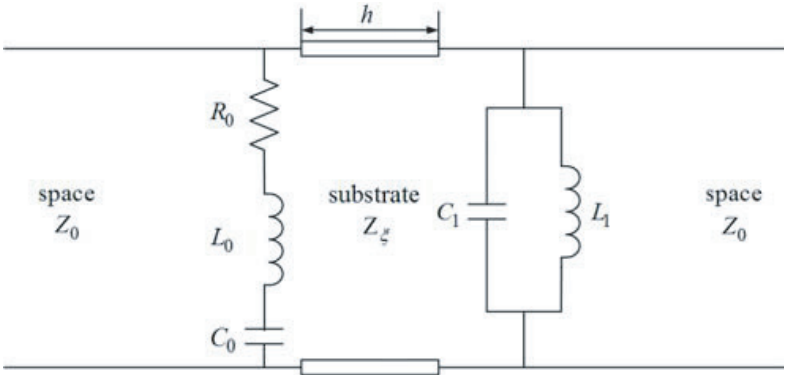

Figure 1. The equivalent circuit of radome.

2.1. Transmission Matrix in Passband

When the characteristic impedance of substrate is equal to that of free space ($Z_\xi = Z_0$), the transmission coefficient S_{21} of radome within passband may be calculated as (1).

$$S_{21} = 1 - \frac{A}{C} + j\frac{B}{C} \tag{1}$$

where

$$\begin{aligned} A &= \omega_p^2 C_0^2 Z_0 (2R_0 + Z_0) \\ B &= 2\omega_p C_0 Z_0 (1 - \omega_p^2 L_0 C_0) \\ C &= 4(1 - \omega_p^2 L_0 C_0)^2 + \omega_p^2 C_0^2 (2R_0 + Z_0)^2 \end{aligned}$$

In Equation (1), $\omega_p (\omega_p = 1/\sqrt{L_1 C_1})$ represents the angular frequency corresponding to transmitting frequency. Both the loaded resistance and impedance of free space are about several hundred ohms. By analyzing Equation (1), it is found that when the resonant frequency of resistive FSS is equal to that of bandpass FSS, minimum value of the transmission coefficient S_{21} is obtained. Hence the resonant frequency of resistive FSS should keep off that of bandpass FSS in order to transmit more power.

2.2. Reflection Coefficients in Absorptive Band

When the incident wave is located in the absorptive band, the bandpass FSS may be treated as a metal plate [1]. So the impedance Z_r of radome may be expressed as Equation (2).

$$Z_r = R_r + jX_r \tag{2}$$

where

$$R_r = \frac{\omega^2 Z_\xi^2 C_0^2 R_0 \tan^2 \beta h}{(1-\omega^2 L_0 C_0 - \omega Z_\xi C_0 \tan \beta h)^2 + \omega^2 R_0^2 C_0^2}$$

$$X_r = \frac{-\omega Z_\xi^2 C_0 \tan^2 \beta h + \omega^2 R_0^2 C_0^2 Z_\xi \tan \beta h + Z_\xi \tan \beta h (1-\omega^2 L_0 C_0)}{(1-\omega^2 L_0 C_0 - \omega Z_\xi C_0 \tan \beta h)^2 + \omega^2 R_0^2 C_0^2}$$

where β is phase shift constant in substrate.

In order to minimize the reflection coefficients, the impedance Z_r of radome should match that of the free space [12]. By analyzing Equation (2), it is found that a thinner substrate with a lower permittivity will shift the starting frequency of the absorptive band to a higher frequency. If the thickness becomes too thin, the coupling effect between the bandpass FSS and the resistive FSS may become strong, which may degrade the absorbing property.

Equations (1) and (2) are obtained at the condition of simplest case of radome. For specific structures, the equivalent circuit of resistive and bandpass FSS may be reconstructed.

3. DESIGN AND SIMULATION

With the aid of the theoretical insights provided in Section 2, the novel radome is designed. Concentric double square rings with resistors loaded are used as resistive FSS and interdigital square loops as bandpass FSS. In order to reduce the simulated time greatly, the period of resistive FSS is equal to that of bandpass FSS. Both resistive FSS and bandpass FSS are polarization independent structures. The configuration of the designed radome is shown in Fig. 2.

The dimensions of the unit cell of radome are presented in Table 1. The optimized resistances loaded on outer and inner loops are 300Ω and 1000Ω, respectively. Fig. 3 shows the simulated results when transverse electric (TE) wave is normal incidence in CST. The boundaries of X and Y direction are set as unit cell and that of Z direction set as open (add space), where X, Y and Z represent the Cartesian spatial coordinates in CST. Z direction is the direction of wave travel. The material of substrate is selected as free space.

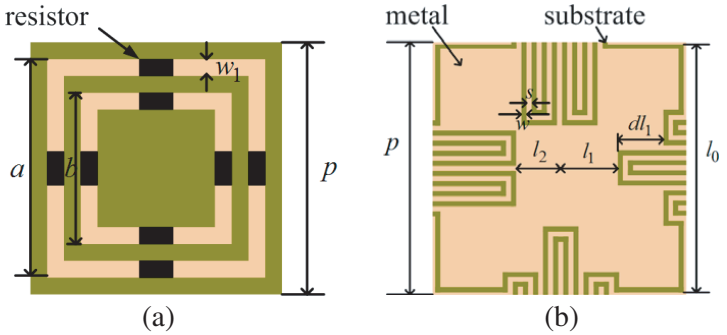

Figure 2. The configuration of miniaturized radome, (a) resistive FSS, (b) bandpass FSS.

Table 1. The parameters list for radome.

parameters	p	l_0	l_1	l_2	dl_1	w	w_1	s	a	b
Value (mm)	10	9.8	2.5	2	1.5	0.2	1	0.2	8.5	5.5

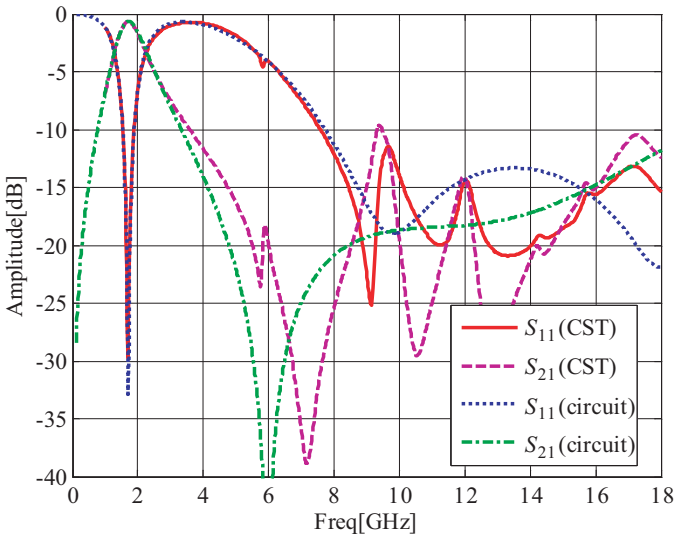

Figure 3. Simulated transmission and reflection coefficients.

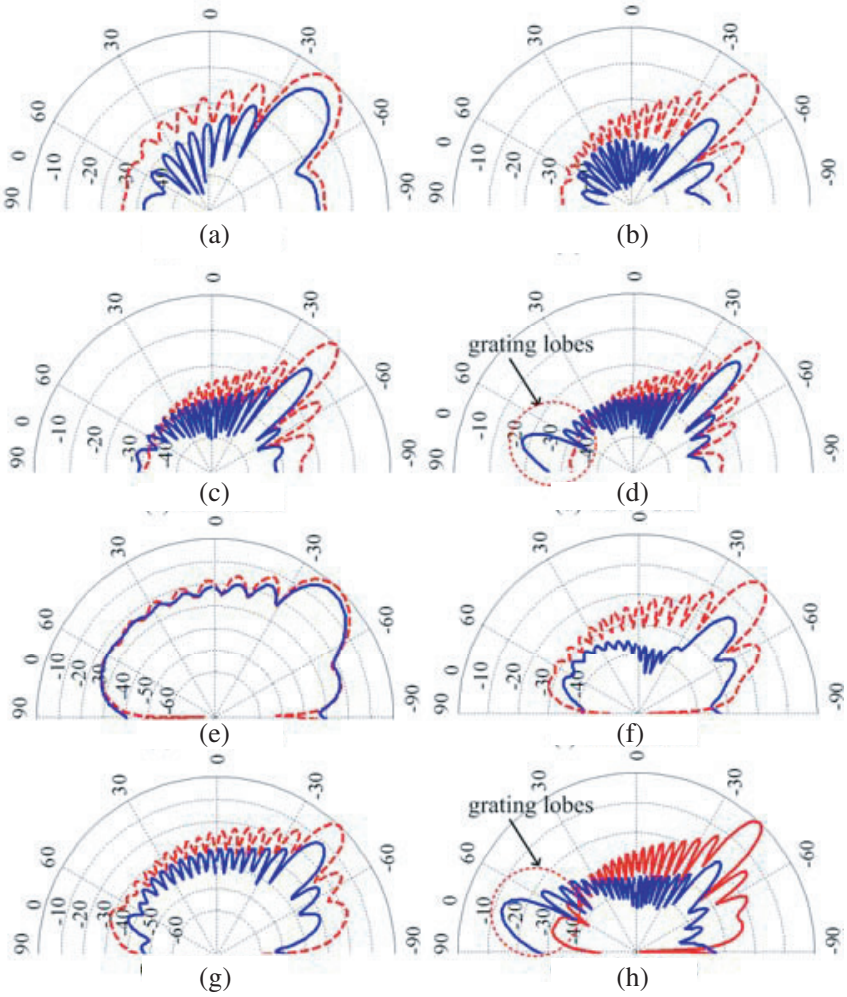

Figure 4. Bistatic reflection of radome and metal sheet. (a) TE 7 GHz, (b) TE 12 GHz, (c) TE 15 GHz, (d) TE 18 GHz, (e) TM 7 GHz, (f) TM 12 GHz, (g) TM 15 GHz, (h) TM 18 GHz.

As shown in Fig. 3, the passband locates at 1.7 GHz, and the −10 dB absorbing band ranges from 7.5 GH to over 18 GHz. From Fig. 3, it is also found that the grating lobes are shifted out of absorbing band to higher frequency. The difference of results obtained from CST and equivalent circuit may owe to that the equivalent circuit of interdigital square loops is hard to construct precisely.

Figure 4 shows the comparisons of the bistatic reflection coefficients between the metal and the radome obtained through simulation in CST. Both sheets are 200 mm × 200 mm, and the incident angle of both TE and transverse magnetic (TM) in CST is 45°. The boundaries of X, Y and Z directions are the bistatic reflections of the metal sheet and radome, respectively. The results shown in Fig. 4 are maximum normalized using maximum reflected power of metal sheet, and the unit of radius is dB. Compared to the metal sheets, the bistatic reflections of the radome are reduced obviously, especially in the specular direction for both TE and TM modes. From Fig. 4(d) and Fig. 4(h), it is found that the grating lobes appear when the incident angle is 45° at 18 GHz. In order to guarantee the performance, the radome should be applicable to frequencies below 18 GHz.

4. EXPERIMENTAL RESULTS

In order to verify the transmission and absorbing properties, a prototype, as shown in Fig. 5, is fabricated using the technology of printed circuit board. The dimension of the sample is 300 mm × 300 mm. The sample contains 30 × 30 unit cells. Both the resistive and bandpass FSS are printed on the Rogers Ro4350 ($\xi_r = 3.48$ and thickness 0.25 mm). The PMI foam ($\xi_r = 1.12$ and thickness 4 mm) is used as the substrate.

Figure 6 shows a photograph of measurement setup. A wooden fixture, covered with RF absorbing material and windowed at center, is located in the middle of two ridged horn antennas. The fabricated radome is put at this window when measured. The side length of wooden fixture is 1.5 m. The operation band of horn antenna is $1 \sim 18$ GHz. The distance between fixture and horn antenna is 0.6 m to ensure that the radome is excited by plane wave. The vector network analyzer (VNA) Anritsu Ms4642A is used to measure the transmission and reflection coefficients of radome. The output power of VNA is set to high, ranging from −3 dBm to 3 dBm. The incident angle can be adjusted by changing the direction and position of antenna.

Figure 7 shows the transmission and reflection coefficients of radome under the condition of different incident angles and polarization directions. The measured passband is located at around 1.7 GHz and agrees well with the simulated one. The large difference of reflection coefficients between simulations and measurements may be ascribed to the measurement error. Compared to measurement for the transmission coefficients, the test for reflection coefficient is more sensitive to the experimental arrangement, which is hard to adjust by manual precisely. The reason is that the reflecting power is much lower than transmission ones. The measured absorbing bandwidth is over 10 GHz for both TE and

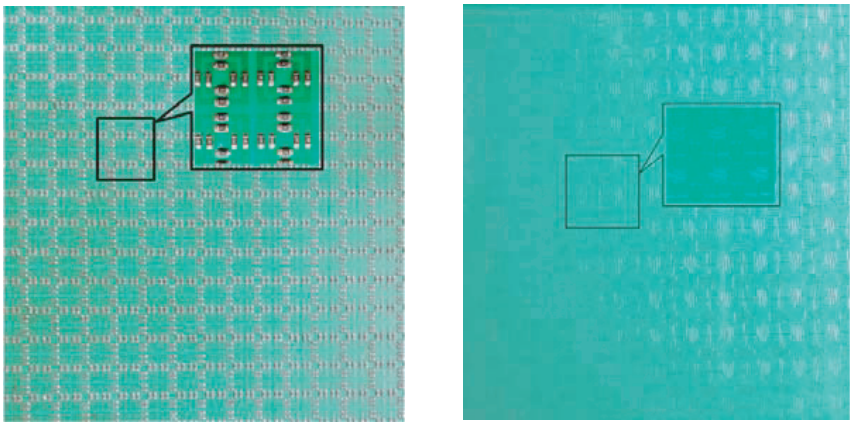

(a) (b)

Figure 5. Photograph of radome prototype, (a) resistive FSS, (b) bandpass FSS.

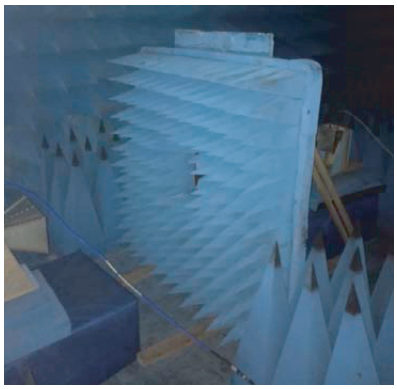

Figure 6. The photograph of measurement setup.

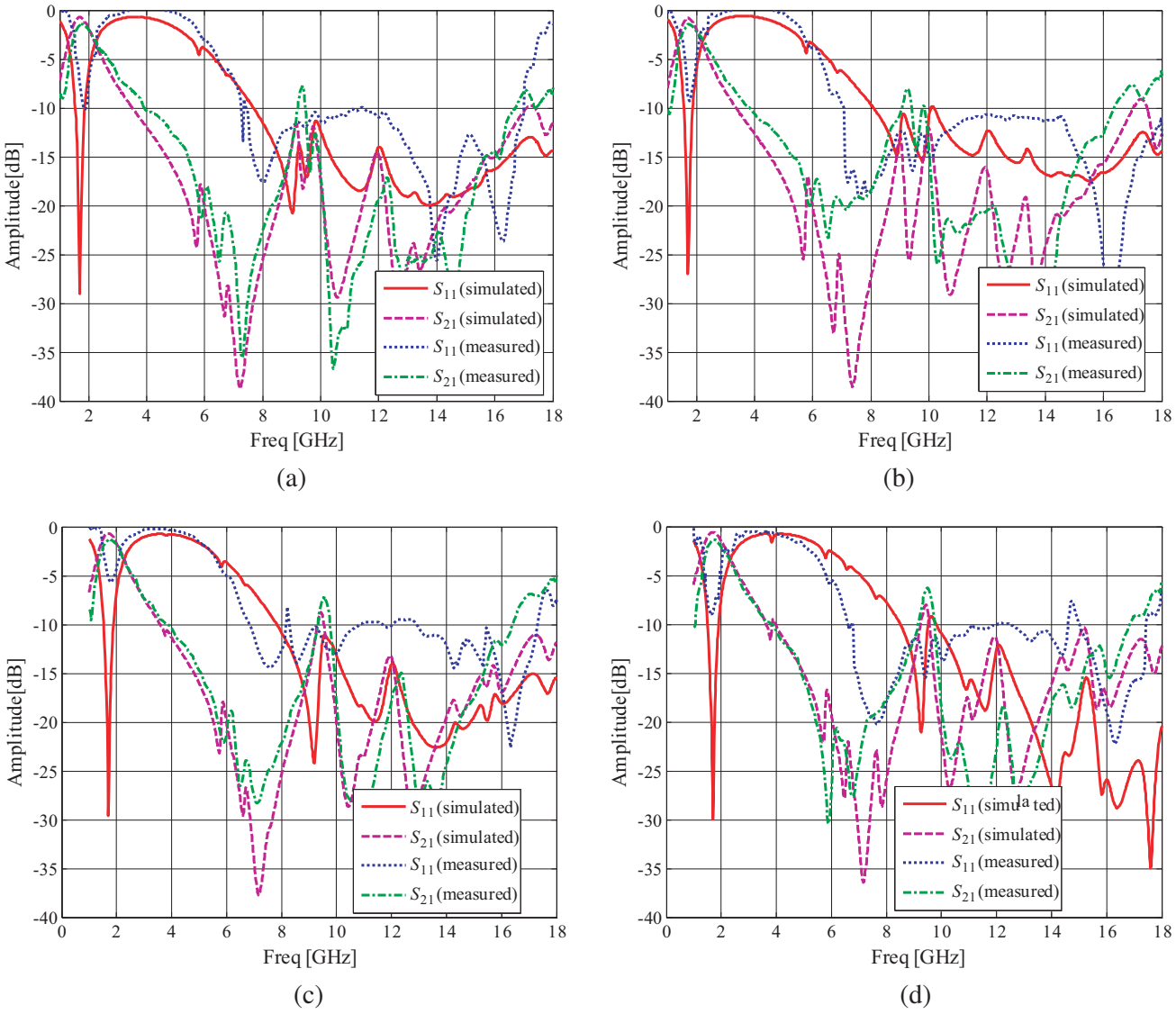

Figure 7. Measured transmission and reflection coefficients of radome. (a) TE 15°, (b) TE 30°, (c) TM 15°, (d) TM 30°.

TM wave incidences. The absorbing and transmission properties keep almost stable as the incident angle increases. Different from the simulated absorbing band, the measured one moves to lower frequency. The differences may owe to the parasitic effects of packaging and measurement errors, especially the reflection coefficient measurement errors.

5. CONCLUSIONS

This paper designs a miniaturized and ultrathin absorptive/transmissive radome based on the interdigital square loops. The thickness of the radome is only 4.5 mm. Both the resistive and bandpass FSS are polarization independent structures, hence the radome is polarization independent. A prototype is fabricated in order to verify the transmission and reflection properties of radome. The experiments show that the transmitting frequency is located at 1.7 GHz, which agrees with the simulated one. The absorptive band is over 10 GHz for both TE and TM incidences. From the simulation, it is found that the grating lobes are shifted out of absorbing band at normal incidence. But when the incident angle increases, the grating lobes appear at 18 GHz. Hence, the frequency suitable for this radome is below 18 GHz.

REFERENCES

1. Costa, F. and A. Monorchio, "A frequency selective radome with wideband absorbing properties," *IEEE Transactions on Antennas And Propagation*, Vol. 60, No. 6, June 2012.
2. Arceneaus, W. S., R. D. Akins, and W. B. May, "Absorptive/transmissive Radome," U.S.Patent 5400,043, May 21, 1995.
3. Liu, L., Y. Li, Q. Meng, W. Wu, et al., "Design of an invisible radome by frequency selective surfaces loaded with lumped resistors," *Chin. Phys. Lett.*, Vol. 30, No. 6, 064101, 2013.
4. Chen, Q. and Y. Fu, "A planar stealthy antenna radome using absorptive frequency selective surface," *Microwave and Optical Technology Letters*, Vol. 56, 1788–1792, 2014.
5. Chen, Q., J. Bai, L. Chen, and Y. Fu, "A miniaturized absorptive frequency selective surface," *IEEE Antennas and Wireless Propagation Letters*, Vol. 14, 80–83, 2015.
6. Zhou, H., L. Yang, S. Qu, et al., "Experimental demonstration of an absorptive/transmissive FSS with magnetic material," *IEEE Antennas and Wireless Propagation Letters*, Vol. 13, 114–117, 2014.
7. Munk, B. A., *Frequency Selective Surfaces: Theory and Design*, Wiley, New York, 2000.
8. Zhang, S., Y. Ying, and X. Ren, "Interdigitated hexagon loop unit cells for wide band miniaturized frequency selective surfaces," *9th International Symposium on Antennas Propagation and EM Theory (ISAPE)*, 770–772, 2010.
9. Costa, F. and A. Monorchio, "Absorptive frequency selective radome," *General Assembly and Scientific Symposium*, 1–4, 2011.
10. Costa, F., A. Monorchio, and G. Manara, "An equivalent circuit model of frequency selective surfaces embedded within dielectric layers," *Proc. IEEE Antennas and Propagation Society International Symposium*, Charleston, SC, June 2009.
11. Costa, F., A. Monorchio, and G. Manara, "Efficient analysis of frequency selective surfaces by a simple equivalent circuit model," *IEEE Antenna And Propagation Magazine*, Vol. 54, No. 4, 35–47, 2012.
12. Han, Y., W. Che, and Y. Chang, "Investigation of thin and broadband capacitive surface based absorbers by the impedance analysis method," *IEEE Transactions on Electromagnetic Compatibility*, Vol. 57, No. 1, 22–26, 2015.